Accepted Manuscript

Elastic wave propagation study in copper poly-grain sample using FEM

Sudhakar Matle

PII: S2095-0349(16)30053-8
DOI: http://dx.doi.org/10.1016/j.taml.2016.09.003
Reference: TAML 106

To appear in: *Theoretical & Applied Mechanics Letters*

Received date: 24 June 2016
Revised date: 24 August 2016
Accepted date: 12 September 2016

Please cite this article as: S. Matle, Elastic wave propagation study in copper poly-grain sample using FEM, *Theoretical & Applied Mechanics Letters* (2016), http://dx.doi.org/10.1016/j.taml.2016.09.003

Highlights

1. Absorbed boundary conditions
2. Wave scattering on shape
3. Elastic wave propagation
4. Orientation effects on grain sample
5. Grain size and random orientation effects

Elastic wave propagation study in copper poly-grain sample using FEM

Sudhakar Matle[a,*]

[a]*School of Advanced Sciences , VIT University, Vellore-632014, INDIA*

Abstract

The paper presents Voronoi based micro-structure modeling through elastic wave propagation in a poly-crystalline copper using finite element method. The micro-structural parameters studied here are; the grain size and the grain orientation. The poly-crystalline copper is modeled as a randomly oriented Voronoi cells in a fixed 2D computational domain. Tone burst 3-cycle pulse of 1MHz frequency is used as the line source or point source for testing. Welded contact conditions are used at the interface boundaries of any two mutual cells of the domain. It is reported that wave scattering independent of the shape when the size of the scatterer less than the wavelength. Also, It is concluded that transmission efficiency increases as the cell size decreases

Key words: grain size, random orientation, finite element method, elastic wave propagation.

Nomenclature

x, y	cartesian coordinates
u_x	displacement in x-direction (m)
u_y	displacement in y-direction(m)
u	displacement field(m)
t	time (s)
c	velocity of sound (m/s)
N	total number of cells
A	size of the domain (m^2)
d	average grain size $(\sqrt{\frac{A}{N}}, m)$
λ_N	a dimension less quantity$(=\frac{\lambda}{d})$
n_{ed}	number of element degrees of freedom

[1] [a]Corresponding author.: Sudhakar Matle
[2] +0091- 9840269197 (Matle)
[3] Email addresses : iitsudha@gmail.com (Sudhakar Matle)

N_a, N_b	shape functions
B_a, B_b	$\nabla N_a, \nabla N_b$
k^e	stiffness matrix of the e^{th} element
K	stiffness matrix
d_p	distance between point sources(=0.000325m)

Suffixes

a, b	element node numbers
r	$n_{ed}(a-1)+i$
s	$n_{ed}(b-1)+j$

Greeks

ρ	density of the material (kg/m^3)
σ	Cauchy stress tensor
ϵ	infinitesimal elastic strain tensor
κ	wave number (m^{-1})

1 Introduction

Micro-structural study is of particular importance because of the grain boundary effects, deformation due to loading and boundary impact in reinforcement of the material. For instance, the copper metal (used in semi-conductor manufacturing) which is highly anisotropic as a single crystal possess a microstructure [1]-[2] wherein the sample is decomposed into smaller grains. The atoms in individual grains exist in crystal lattice and the lattice orientations of the adjacent grains differ. This type of anisotropy[3]-[4] affects the grain boundary interface and in turn causes irregular texture (dislocations) in polycrystals.

At micro-scale, wave scattering in poly-crystals is directional dependent, frequency dependent and damage dependent for shear horizontal and quasi longitudinal waves. The practical applications are; characterization of defects, material structure and stress determination in textured components. Knowledge of interaction of waves with defects is the key for the development of NDT (non-destructive testing) inspection techniques. Researchers conducted experiments on wave propagation[5] in a poly-crystalline materials. Zhang et.al.[6] measured the ultrasonic attenuation as a function of frequency and the average grain size in copper and copper-aluminum samples. Maurel et.al. [7] address the elastic wave propagation through the 2D poly-crystal with the assumption that the source of scattering due to grain boundaries interaction and obtained good approximation for low-angle boundaries. Stanke and Kino [8] used perturbation method to solve for attenuation, phase velocity variations of elastic

waves in single-phase, poly-crystalline media.

A discrete approach is needed to model how the waves interact with interface discontinuities, including structural features, cracks, corrosion and other forms of defects. Finite element methods[9] have been used to model a wide range of bulk and guided wave problems and have successfully provided important information about wave interaction with discontinuities[10–12]. However, no one has presented the elastic wave propagation in crystal at micro scale in terms of the grain size and the grain orientation using finite element method.

The paper is organized as follows. In section 2 a brief description of the modeling the crystal and mathematical formulation of the problem are reported. Numerical scheme and description of the method are presented in section 3. Brief results and conclusions are reported in the section 4.

2 Mathematical model

Copper grain sample is modeled as a 2D computational domain composed of Voronoi cells and it is schematically sketched in Fig.1 and Fig.2 . The average grain size(A) is defined as ratio of the total size $0.05m \times 0.05m$ to the number of cells in the computational domain. In order to define elastic wave propagation, the following input parameters are required. Elastic constants of the copper crystal at 298K are; $c_{11} = 1.683 \times 10^{11} N/m^2, c_{12} = 1.221 \times 10^{11} N/m^2$ and $c_{44} = 0.757 \times 10^{11} N/m^2$. Density of the copper is $8932 kg/m^3$.

2.1 Governing equations

The wave equation of motion for a 2D computational domain Ω is given by

$$\rho \frac{\partial^2 u}{\partial t^2} = \nabla \cdot [c]\epsilon \quad on \quad \Omega_j, j = 1, 2, ...n_c \tag{1}$$

where $[c]$ is the elasticity matrix. Since each cell is rotated randomly by an angle θ about the z-axis in counter clock wise direction, then the transformed elasticity matrix $[c^p]$ is written as follows.

$$[c^p] = M[c]M^t \tag{2}$$

where Bond stress transformation matrix M is given by

$$[M] = \begin{pmatrix} cos^2\theta & sin^2\theta & 0 & 0 & 0 & sin2\theta \\ sin^2\theta & cos^2\theta & 0 & 0 & 0 & -sin2\theta \\ 0 & 0 & 1 & 0 & 0 & 0 \\ 0 & 0 & 0 & cos\theta & -sin\theta & 0 \\ 0 & 0 & 0 & sin\theta & cos\theta & 0 \\ -\frac{sin2\theta}{2} & \frac{sin2\theta}{2} & 0 & 0 & 0 & cos2\theta \end{pmatrix} \tag{3}$$

in Voigt notation

$$[c^p] = \begin{pmatrix} c^p_{11} & c^p_{12} & c^p_{13} & 0 & 0 & c^p_{16} \\ c^p_{12} & c^p_{11} & c^p_{13} & 0 & 0 & -c^p_{16} \\ c^p_{13} & c^p_{13} & c^p_{33} & 0 & 0 & 0 \\ 0 & 0 & 0 & c^p_{44} & 0 & 0 \\ 0 & 0 & 0 & 0 & c^p_{44} & 0 \\ c^p_{16} & -c^p_{16} & 0 & 0 & 0 & c^p_{66} \end{pmatrix} \tag{4}$$

$$\begin{aligned} c^p_{11} =& c_{11} - (\frac{c_{11} - c_{12}}{2} - c_{44}) sin^2 2\theta \\ c^p_{12} =& c_{12} + (\frac{c_{11} - c_{12}}{2} - c_{44}) sin^2 2\theta \\ c^p_{13} =& c_{12} \\ c^p_{16} =& -(\frac{c_{11} - c_{12}}{2} - c_{44}) sin 2\theta cos 2\theta \\ c^p_{33} =& c_{11} \\ c^p_{44} =& c_{44} \\ c^p_{66} =& c_{44} + (\frac{c_{11} - c_{12}}{2} - c_{44}) sin^2 2\theta \end{aligned}$$

2.2 Boundary conditions

In order to complete description of the problem, we need a boundary condition on the boundary of Ω, denoted by $\partial\Omega$. The source of excitation is employed at the left end while free or absorbed boundary conditions are used at the remaining three boundaries of the $\partial\Omega$. Tone burst 3-cycle pulse of 1MHz frequency is used as the operating point source or line source for testing. Duration of the pulse excitation is $10^{-6}s(1/f)$. Mathematically, it is written as

$$u_s = 0.5\Big(1 - cos\Big(\frac{2\pi f}{3}\Big)\Big) cos(2\pi f t)(t < 10^{-6}) \tag{5}$$

where u_s, displacement source and f, frequency of excitation (1MHz) respectively. Also, we need to make precise how the displacement and stress fields on the different sub domains Ω_j are related across the interfaces with various elastic properties. Local continuity of the displacement and the traction at the interface ensures that the global displacement function solves the elastic wave propagation problem. Initially, the displacement is zero at 293K throughout the computational domain.

3 Numerical scheme

To demonstrate the normal and the tangential component of the displacement and the traction are continuous along the interface boundaries, we define the "jump" in displacement and traction are as follows.

$$\begin{aligned}
[u_n] =&(u_i^+ - u_i^-)n_i^+ \\
[u_t] =&(u_i^+ - u_i^-)t_i^+ \\
[\sigma_{in}] =&(\sigma_{ij}^+ - \sigma_{ij}^-)n_i^+ \\
[\sigma_{it}] =&(\sigma_{ij}^+ - \sigma_{ij}^-)t_i^+
\end{aligned} \tag{6}$$

where n_i^+ and t_i^+ are the unit normal and unit tangential in +-ve directions respectively. The problem is to find $u_i : \bar{\Omega} \rightarrow R$ such that

$$\begin{aligned}
\rho u_{i,tt} =&[c^p]\epsilon_{ij,j} \quad \text{on} \quad \Omega \times [0,T) \\
[u_n] =&0 \quad \text{on} \quad \Gamma_{int} \\
[u_t] =&0 \quad \text{on} \quad \Gamma_{int} \\
[\sigma_{in}] =&0 \quad \text{on} \quad \Gamma_{int} \\
[\sigma_{it}] =&0 \quad \text{on} \quad \Gamma_{int} \\
u_i(\bar{x},0) =&0, \quad \bar{x} \in \Omega \\
u_{i,t}(\bar{x},0) =&0, \quad \bar{x} \in \Omega \\
u_i =&0 \quad \text{on} \quad \Gamma_{out} \times [0,T) \\
u_i =&u_s \quad \text{on} \quad \Gamma_{in} \times [0,T)
\end{aligned} \tag{7}$$

where $\Gamma_{in}, \Gamma_{out}$ and Γ_{int} are incident, outer and interface boundaries respectively. The weak formulation of the problem is to find $u \in H^1(\Omega)$ such that for $w \in L_2(\Omega)$

$$(w, \rho u_{,tt}) + a(w,u) = (w, u_s) \tag{8}$$

where

$$\begin{aligned}
a(w,u) =& \int_\Omega \epsilon(w)^T [c^p] \epsilon(u) d\Omega \\
(w, \rho u_{,tt}) =& \rho \int_\Omega w u_{,tt} d\Omega \\
(w, u_s) =& \int_\Gamma w u_s d\Gamma.
\end{aligned}$$

Then the Galerkin finite element formulation is used to find $u^h \in H_1(\Omega^h)$ such that for $w^h \in L_2(\Omega^h)$

$$(w^h, \rho u^h_{,tt}) + a(w^h, u^h) = (w^h, u_s) \quad \text{on} \quad \Omega^h \times [0,T) \tag{9}$$

Then eq.9 leads to the following matrix problem. Given $f \in [0,T) \rightarrow R^{n_{eq}}$, find $u \in [0,T) \rightarrow R^{n_{eq}}$ such that

$$\begin{aligned} Qu_{,tt} + Ku &= f, \quad t \in [0, T) \\ u(0) &= 0 \\ u_{,t}(0) &= 0 \end{aligned} \tag{10}$$

where

$$\begin{aligned} Q &= \sum_{i=1}^{n_{el}} (q^e) \\ q^e &= [q^e_{rs}] \\ q^e_{rs} &= \delta_{ij} \int_{\Omega^e} N_a \rho N_b d\Omega \\ K &= \sum_{i=1}^{n_{el}} (k^e) \\ k^e &= [k^e_{rs}] \\ k^e_{rs} &= e_i^T \int_{\Omega^e} B_a^T [c^p] B_b d\Omega e_j \\ f &= \sum_{i=1}^{n_{el}} (f^e) \\ f^e &= [f^e_{rs}] \\ f^e_{rs} &= \int_{\Omega^e} N_a u_s d\Omega \end{aligned}$$

Then time discretization by Newmark implicit finite difference scheme of the eq.10 leads to the following.

$$\begin{aligned} Qu^2_m + Ku^0_m &= f_m \\ u^0_m &= u^0_{m-1} + \delta t u^1_{m-1} + \frac{1}{4}(u^2_{m-1} + u^2_m) \\ u^1_m &= u^1_{m-1} + \frac{1}{2}\delta t (u^2_{m-1} + u^2_m) \end{aligned} \tag{11}$$

where $u^0_m = u(t_m), u^1_m = u_{,t}(t_m), u^2_m = u_{,tt}(t_m), f(t_m) = f_m, \delta t = 5 \times 10^{-7}$s.

4 Results and discussion

In this section, results on absorbed boundary, wave scattering around the scatterer, elastic wave propagation in copper grain sample with various orientations and computation of transmission coefficients for various grain sizes and various grain random orientations are presented.

4.1 Wave propagation in a domain with absorbed boundary conditions

Firstly, wave equations are solved in a domain with perfect matched layer conditions using hybridized finite element method. The average finite element size in a non-uniform mesh consists of quadratic triangular elements is taken as '$\frac{\lambda}{12}$'. Fig.3(a) shows the wave propagation in a frequency domain. It is

observed that 3-cycle wave is almost absorbed at the boundaries of the domain. Fig.3(b) shows the total displacement field profiles against the frequency at the probe of the domain with and without PML boundaries. It indicates that the amplitude lies in between -1 and 1 for the profile with PML boundary due to no reflections.

4.2 shape independency of the scatterer

In order to demonstrate scattering behavior in linear elastic copper medium, an aluminum object of size less than the wavelength is considered. The distance from the line source of excitation to the object of interest is $\frac{D^2}{4\lambda}$, where 'D' is the length of the line source and 'λ' is the wave length of the copper medium. The distance from the object to the probe opposite to the source boundary is $\frac{d_1^2}{4\lambda}$, where 'd_1' is the diameter of the object. Fig.4 shows that wave displacement profiles around the scattering object of various shapes, namely, hexagon and circular respectively. From the plot, it clears that profiles of hexagon and circular objects are coincident and thus scattering does not depend on the object shape when its size less than the wave length.

4.3 Elastic wave propagation in cells with orientation

The computational domain composed of 27 cells is considered for present study. The source of excitation is at the center of the domain. Fig.5(a) shows the pseudo plot of the elastic wave propagation in terms of displacement at time $2.5 \times 10^5 s$. Here the angle of orientation of the each cell is fixed at 45^o. From the plot, it is observed that there are no significant disturbances for the elastic waves at the interfaces of the domain. Fig.5(b) shows the pseudo plot of elastic wave under the same input conditions mentioned above but orientation angles of any two mutual cells are different. From the plot, it is observed that shear wave is distorted and splits into two quasi shear waves at the interfaces due to irregularity. It is concluded that the orientation caused anisotropy impacted the elastic wave propagation considerably.

4.4 Elastic wave propagation in cells with random orientation

In order to demonstrate orientation effects on the elastic wave thoroughly, an array of nine time delayed ($\Delta t_n = \frac{nd_p}{c} sin\theta_1, n = 1, 2, ..., 9$) point sources separated by fixed aperture are considered at the top of the domain. The steering angle θ_1 is taken as 15^o. Fig.6 shows the pseudo plot of displacement in y-direction in copper sample with 220 grain cells. it clears that quasi longitudinal and shear are distorted at the very beginning due to anisotropy caused random orientation.

4.5 Evaluation of transmission coefficients

Transmission coefficient (Tc) is defined as the ratio of the fast Fourier transform of the amplitude of the signal at the probe point near the boundary opposite to the source boundary to the fast Fourier transform of the amplitude of the incident signal. Fig.7 shows transmission coefficient against frequency for various cell sizes and various random orientations. From the plot, it is clear that transmitted signal has distortions ($Tc >> 1$) at low range frequencies

starting from 50KHz to 75KHz when the cell has fixed random orientation (λ_1) and λ_N less than 2. Signal distortions are minimized and ultimately the anisotropy poly-grain copper behaves on an average as an isotropy crystal when the value of $\lambda_N >> 2$.

5 Conclusion

In view of results and discussions, the following conclusions are drawn.

- Developed a micro-structural model for poly-crystalline material explicitly using finite element method.
- Elastic wave interactions with material interface boundaries have been investigated.

Acknowledgment

The corresponding author is very thankful to BRNS project for their financial support and IGCAR kalpakkam for their valuable discussions on this work.

References

[1] A. Kuprat , "Modeling microstructure evolution using gradient weighted moving elements", *SIAM J.Sci.Comput.*, vol. 22, no. 2, pp. 535-560, 2000.

[2] I. Benedetti and M.H. Aliabadi, "Multi-scale modeling of poly-crystalline materials: A boundary element approach to material degradation and fracture", *Comput.Methods in Appl.Mech.Engrg.*, Vol.289, pp.429-453, 2015.

[3] H. Hallberg, "Influence of anisotropic grian boundary properties on the evolution of grain boundary character distribution during grain growth-A 2D level set study", *Modeling and Simulation in Mathematical Science and Engineering*, Vol.22,8, pp.085005, 2014.

[4] H. Fang, K. Matsumoto, T. Sumigawa and T. Kitamura," Anisotropic elastic properties of chiral sculptured thin films at micro-scale evaluated resonance frequency spectra", *Eurpean Journal of Mechanics A/Solids*, Vol. 49, pp.510-517, 2015.

[5] B.R. Thompson, "Elastic wave propagation in random poly-crystals, fundamentals and applications to non-destructive testing evaluation", *Imaging of Complex Media with Acoustic and Seismic Waves*, Vol.84, pp.233-257, 2002.

[6] X.G. Zhang, W.A. Simpson (Jr.), J.M. Vitek, D.J. Barnard, L.J. Tweed and J. Foley, "Ultrasonic attenuation due to grain boundary scattering in copper and copper-aluminum", *Journal of Acoustical Society of America*, Vol.116, pp.109, 2004.

[7] A. Maurel, V. Pagneux, D. Boyer and F. Lund, "Propagation of elastic waves through poly-crystals: The effects of scattering from dislocation arrays", *Proceedings of the Royal Society A*., Vol.462, 2073, pp.2607-2623, 2006.

[8] F.E. Stanke and G.S. Kino,“ A unified theory for elastic wave propagation in poly-crystalline materials”, *J.Acoust.Soc.Am.*, Vol.75, 665, 1984.

[9] G. Ghosal and J.A. Turner, “Numerical model of longitudinal wave scattering in poly-crystals”, *IEEE Transactions on Ultrasonic Ferro Electrics and Frequency Control*, Vol.56, 7, 2009.

[10] K.A.Graff(Ed.), Wave Motion in Elastic Solids, 1991.

[11] B.A.Auld (Ed.), Acoustic fields and waves in solids, 1973.

[12] W.L.Schmerr(Jr.)(Ed.), Fundamentals of Ultrasonic Non-Destructive Evaluation- A Modeling Approach, 1998.

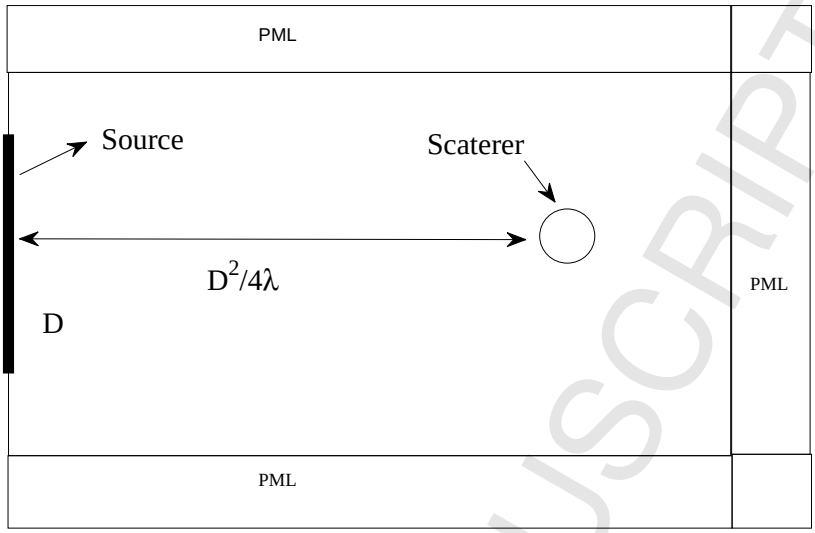

Fig. 1. Schematic sketch of the computational domain

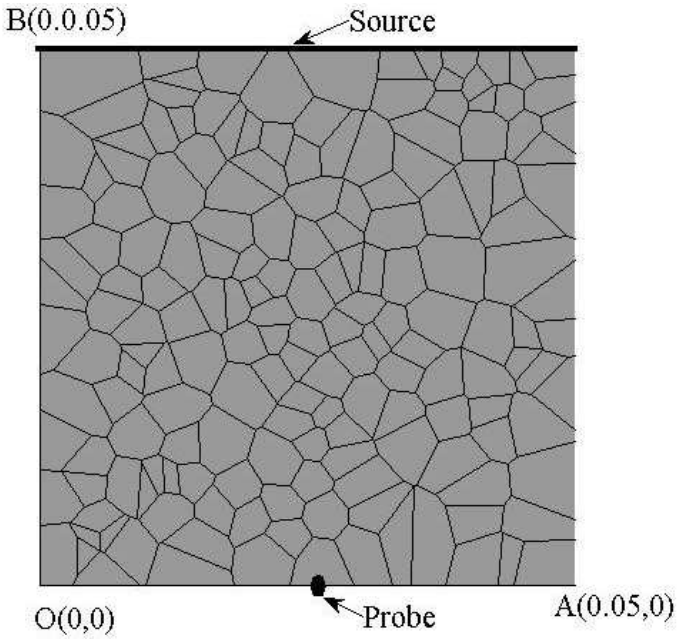

Fig. 2. Voronoi diagram

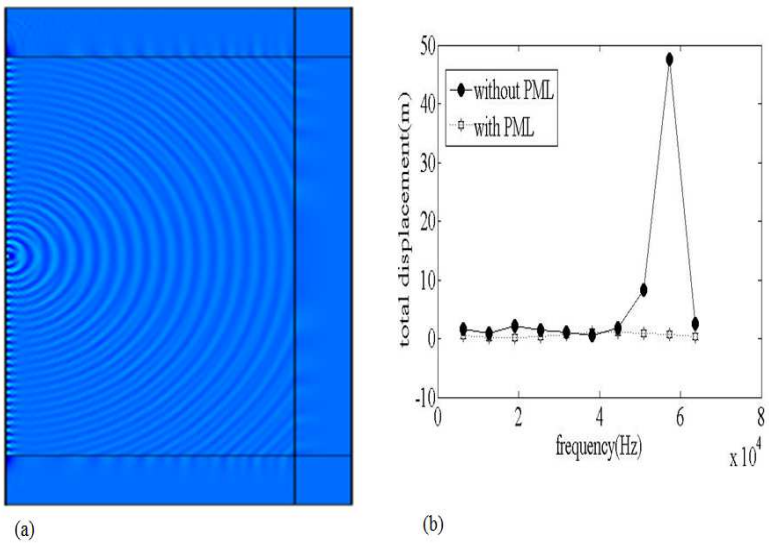

Fig. 3. (a)Wave propagation in a domain with absorbed conditions(b) comparison of displacement profiles with and without absorbed conditions

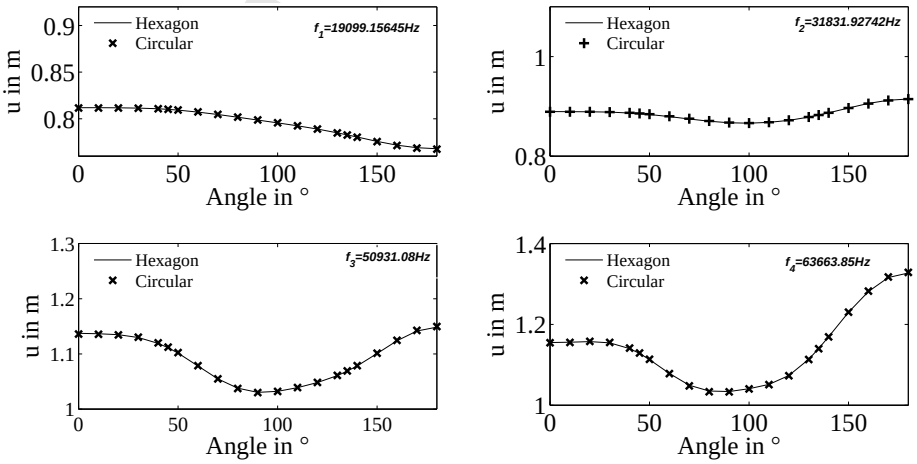

Fig. 4. Shape independency

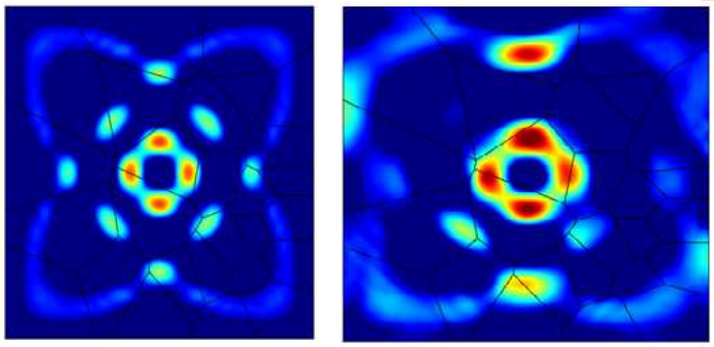

Fig. 5. (a) Elastic wave propagation in cells with equal orientation angle (b) cells with different angles of orientation but not random

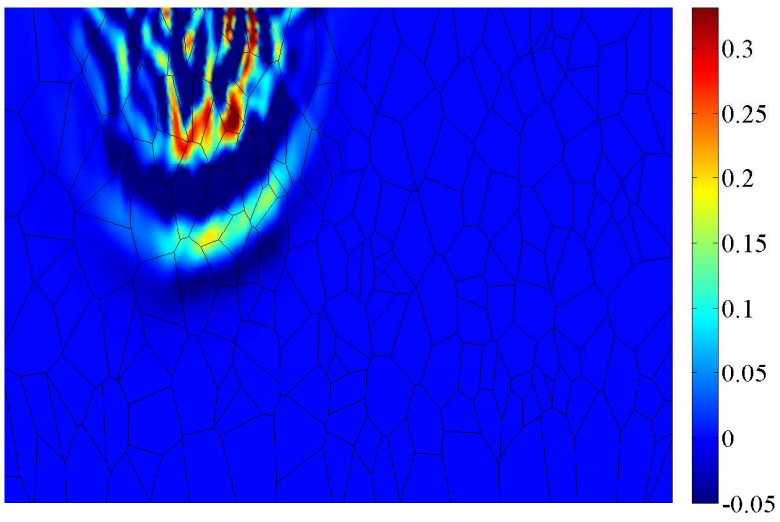

Fig. 6. Pseudo plot of the displacement in $y-$ direction in copper grain sample

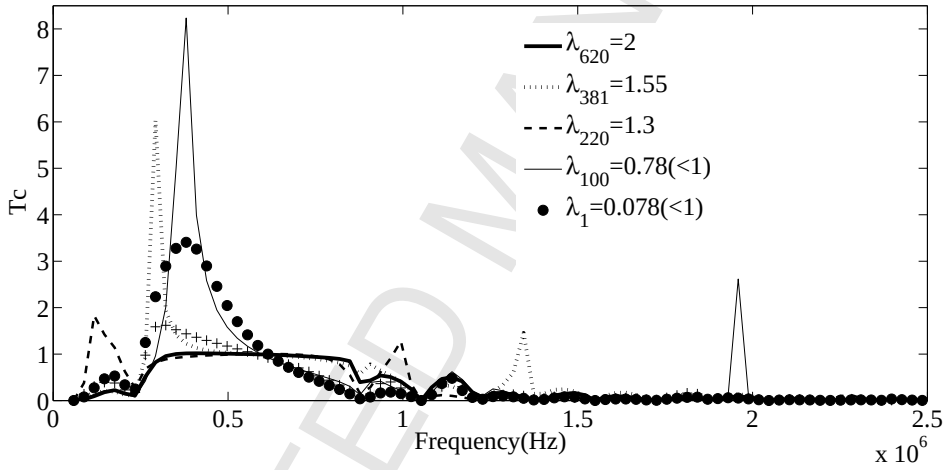

Fig. 7. Transmission coefficient against frequency for various cell sizes